Advanced Functional Materials, Volume 23, Issue 23, pages 2987–2992, June 20, 2013

Submitted to ADVANCED FUNCTIONAL MATERIALS

DOI: 10.1002/adfm.((please insert DOI)

Giant electrocaloric effect in nano-scaled antiferroelectric and ferroelectric phases coexisted relaxor $Pb_{0.8}Ba_{0.2}ZrO_3$ thin film at room temperature

By ***Biaolin Peng***, ***Huiqing Fan***** and ***Qi Zhang*****

Dr. Q. Zhang
Department of Manufacturing and Materials
Cranfield University
Cranfield, Bedfordshire, MK43 0AL, United Kingdom
E-mail: q.zhang@cranfield.ac.uk

Prof. H. Fan
State Key Laboratory of Solidification Processing
School of Materials Science and Engineering
Northwestern Polytechnical University, Xi'an 710072, China
E-mail: hqfan3@163.com

Keywords: $Pb_{0.8}Ba_{0.2}ZrO_3$ thin film; relaxor; field-induced; electrocaloric effect

Recently large electrocaloric effects (ECE) (ΔT = 12 K and ΔS = 8 $JK^{-1}kg^{-1}$ at 776 $kVcm^{-1}$) in antiferroelectric sol-gel $PbZr_{0.95}Ti_{0.05}O_3$ thin film and (ΔT = 12.6 K and ΔS = 60 $JK^{-1}kg^{-1}$ at 2090 $kVcm^{-1}$) in ferroelectric polymer P(VDF-TrFE)55/45 thin film were observed near their ferroelectric Curie temperatures 495 K and 353 K, respectively. Here authors demonstrate a giant EC effect (ΔT = 45.3 K and ΔS = 46.9 $JK^{-1}kg^{-1}$ at 598 $kVcm^{-1}$) in relaxor ferroelectric $Pb_{0.8}Ba_{0.2}ZrO_3$ (PBZ) thin film fabricated on $Pt(111)/TiO_x/SiO_2/Si$ substrate by a sol-gel method, in which nano-scaled antiferroelectric (AFE) and ferroelectric (FE) phases coexist, at room temperature (290 K) rather than at its Curie temperature (408 K). The giant ECE in such a system is attributed to the coexistence of AFE and FE phases and field-induced nano-scaled AFE to FE phase transition. The giant ECE of PBZ thin film makes it a promising material for the application in cooling systems near room temperature.

1. Introduction

ECE is a change in temperature (ΔT) in a polarable material by virtue of the change in entropy (ΔS) upon the application or withdraw of an electric field under adiabatic conditions.[1-3] Simulation results[4] indicate that cooling devices based on large ECE can have much higher

coefficient of performance (COP) (> 60% of Carnot efficient) than those (< 20% of Carnot efficient) of mechanical vapor compression cycle cooling devices such as refrigerator and air-conditioner, which generate strong greenhouse gases during their operations. The bottle neck for development of ECE cooling technologies in the past is that only small ΔT and ΔS can be induced in bulk materials such as only ΔT = 2.5 K and ΔS = 0.2 $JK^{-1}kg^{-1}$ at 750 V in $Pb_{0.99}Nb_{0.02}(Zr_{0.75}Sn_{0.20}Ti_{0.05})O_3$ ceramics[5] because of the restriction of breakdown fields (~ 50 $kVcm^{-1}$).

Recently, by resorting to a thin-film geometry, giant ECE (ΔT = 12 K and ΔS = 8 $JK^{-1}kg^{-1}$ at 776 $kVcm^{-1}$) in the antiferroelectric $PbZr_{0.95}Ti_{0.05}O_3$ (PZT) was observed by Mischenko et al.[1] near antiferroelectric to paraelectric phase transition temperature (T_c = 500 K). This has triggered a new wave of interest in the search of new ECE materials, which results in significant progress in this field and raises hopes for successful development of ECE solid-state cooling units. For example, Saranaya et al. [6] reported a bigger ECE temperature change (ΔT = 31 K) at 413 K and 747 $kVcm^{-1}$ in $Pb(Mg_{1/3}Nb_{2/3})_{0.65}Ti_{0.35}O_3$ thin films deposited by PLD. Lu *et al.* also reported a 40 K temperature change at 318 K and 1200 $kVcm^{-1}$ in $(Pb_{0.88}La_{0.08})(Zr_{0.65}Ti_{0.35})O_3$ relaxor thin films (S.G. Lu, B.Rožič, Q. M. Zhang, Z. Kutnijak, X. Li, E. Furman, L. J. Gorny, M. Lin, B. Malič, M. Kosec, R. Blinc and R. Pirc, Appl. Phys. Lett., 2010, 97, 162904). But the application of cooling devices needs maximum EC effect at or near room temperature. In view of this, Neese et al.[3] reported a ECE temperature change (ΔT) of ~ 12.6 K at 2090 $kVcm^{-1}$ in ferroelectric polymer P(VDF-TrFE)55/45 thin film, near room temperature (353 K).

Usually, a large ECE is often considered to occur around the Curie temperature (T_C) of ferroelectrics[1] where the polarization (P) changes with temperature. Through the first-principles-based simulation, Ponomareva[7] et al. predicted that ferroelectrics with multiple transitions can exhibit giant ECE under large electric fields and with the coexistence of both

positive and negative ECE in one material. Moreover, the origin of negative ECE can be traced to the noncollinearity between the electric field and the polarization, which could induce new ways to enhance the electrocaloric efficiency.

In this work, we report a giant ECE (ΔT = 45.3 K and ΔS = 46.9 $JK^{-1}kg^{-1}$ at 598 $kVcm^{-1}$) in a nano-scaled orthorhombic antiferroelectric phase and rhombohedral ferroelectric phase coexisted relaxor $Pb_{0.8}Ba_{0.2}ZrO_3$ thin film prepared by a sol-gel method at room temperature (290 K) away from its Curie temperature (408 K). A new mechanism was introduced to interpret the dramatic ECE.

2. Results and discussions

2.1. Structure

XRD patterns of PBZ thin films fabricated on Pt(111)/TiO_x/SiO_2/Si substrate by a sol-gel method were illustrated in **Fig.1(a)**. Pure and well crystallized perovskite phase PBZ film was achieved after annealed at 750 °C for 30 min. Superlattice reflections with indices (130) and (112) indicate the existence of orthorhombic antiferroelectric phase[8] in the PBZ thin film. Refined lattice parameters for the orthorhombic antiferroelectric (O_{AFE}) phase are determined to be a_O = 5.83612 Å, b_O = 11.72206 Å and c_O = 8.31065 Å by using the software JADE. In addition to the O_{AFE} phase, a rhombohedral ferroelectric (R_{FE}) phase with lattice parameters a_R = 4.12267 Å and α_R = 90.9541 ° can also be detected. The surface micrograph (inset of Fig.1(a)) of PBZ thin film displays a typical rosette structure,[9] which is formed by the lead loss during the heat-treatment process[10,11] and consists of round lighted-colored regions (rosettes) and the dark region between the rosettes. Inside and in between the rosettes, subgrains with average size of 20 nm can also be clearly observed.

To further study the morphology and microstructure of PBZ thin film in details, the TEM characterization was carried out. Numerous dispersed nanocrystals corresponding to those subgrains in the SEM were observed again in the TEM bright field image (Fig.1(b)). In the

inside of some nanocrystals, lamellar nanodomains with about 2 nm wide (see the blue solid circles) and lamellar nanodomains with about 1 nm wide (see the red dot circles) are clearly visible. The latter can be attributed to be the antiferroelectric domains for 1 nm wide close to its cell parameters, which is consistent with the report by Viehland[12] in PZT. Inset of Fig. 1 (b) shows the selected area electron diffraction (SAED) pattern of PBZ thin film. For simplicity, the lattice indices for SAED were labeled as the pseudo cubic structure rather than the orthorhombic or rhombohedral structure. Circular rings correspond to the (111), (220), and (311) plane reflections (from inside to outside), respectively. The discontinuity of diffraction rings indirectly revealed the nanocrystalline characteristics of PBZ thin film.[13] It is well known that the polarization vector for the R_{FE} phase is <111>,[14] and the rotation between neighboring domains depends on the cell angle α. For PZT,[14] the rhombohedral angle α is 91°, and the possible types of domain can be calculated as 109°, 71°, and 180°. The orientation of permissible uncharged walls is {110} for 109°, {001} for 71° and the plane parellel to the polarization vector is 180° domain. According to the refined α value (90.9541°) of the R_{FE} phase and the feature of the SAED pattern of PBZ thin film, lamellar nanodomains with about 2 nm wide probably is due to the exisitence of 180° ferroelectric domains, which needs to be further confirmed by piezoresponse force microscopy (PFM).

Figure 1. (a) XRD patterns and SEM surface image (inset) of the PBZ thin film; (b) TEM image and SAED pattern (inset).

2.2. Dielectric properties

Temperature dependences of dielectric permittivity (ε) and dielectric loss (tan δ) at different frequencies are shown in **Fig 2.(a)**. Although the dielectric permittivity is higher (ε_m ~ 1200) compared with that found in PZT-based compositions, it is rather lower than the sintered bulk PBZ ceramics with the same composition (ε_m ~ 12000).[15,16] This difference can be attributed to small grain size in thin film compared with similar bulk ceramics and due to

substrate constraint.[17-21] Likewise, the maximum dielectric permittivity is observed at 408 K (T_m), rather than at 425 K reported in PBZ bulk material.[15,16] The relaxation observed by the frequency dependence of the dielectric permittivity indicates the existence of defects (small thickness of the film, clamping by the substrate and low annealing temperature), which may contribute to decreasing of permittivity and the shift in T_m comparing with bulk ceramics. Moreover, the AFE-FE transition cannot be detected in the whole temperature range, which is similar to the phenomenon in PZT thin film.[1]

In order to evaluate the ECE in the PBZ thin film, *P-E* loops at 100 Hz were measured at a 5 K interval in the temperature range between 283 K and 418 K. Representative plots of *P-E* loops are shown in Fig. 2(b) and (c). The temperature dependence of the polarization ($P(T)$) at selected electric field values, established from the upper branches of the *P-E* hysteresis loops in E > 0, is presented in the insets of Fig. 2(b) and (c). The solid lines in the inset of Fig. 2(b) and (c) represent cubic-spline interpolation of raw data.

Leakage currents ($I(t)$) measured in the maximum field employed (598 $kVcm^{-1}$) (Fig. 2(d)) were investigated at room temperature 293 K and near the Curie temperature 403 K, respectively. The observed transients persist up to 1000 ms, even beyond which no breakdown occurs after repetitive testing. By contrast, beyond 200 ms breakdown occurs in the PZT thin film.[1] It can be seen that 1.7 nA is an upper bound for the steady-state leakage current. This value yields negligible Joule heating ($<10^{-3}$ K) and does not affect $P(E)$ because currents of hundreds of μA are required to switch the measured polarizations at 100 Hz.

Figure 2. (a) $\varepsilon(T)$ and tan $\delta(T)$ of PBZ thin film; (b) and (c) *P-E* loops at selected temperatures, the inset is $P(T)$ at selected electric field values; (d) leakage current $I(t)$.

2.3. Electrocaloric effect

Reversible adiabatic changes in temperature (ΔT) and entropy (ΔS) for a material of density (ρ) with heat capacity (C) are given[1-3,22,23] by

$$\Delta T = -\frac{1}{\rho}\int_{E1}^{E2}\frac{T}{c}\left(\frac{\partial P}{\partial T}\right)dE, \quad (1)$$

$$\Delta S = -\frac{1}{\rho}\int_{E1}^{E2}\left(\frac{\partial P}{\partial T}\right)dE \quad (2)$$

assuming the Maxwell relation $(\partial P/\partial T)_E = (\partial S/\partial E)_T$. Values of $(\partial P/\partial T)_E$ were obtained from four-order polynomial fits to the cubic-spline interpolation of raw $P(T)$ data extracted from the upper branches of *P-E* loops in E > 0 (see the inset of Fig. 2(b) and (c)). In the temperature range of interest, the heat capacity (C = 330 $JK^{-1}kg^{-1}$) remains constant for Zr-rich lead-based thin film, and the peak associated with the transition is < 10% of the background.[1] Assuming a constant value of C despite an ~ 50% peak[1] resulted in excellent agreement with direct ECE measurements of ΔT in bulk $Pb_{0.99}Nb_{0.02}(Zr_{0.75}Sn_{0.20}Ti_{0.05})_{0.98}O_3$. Therefore, C = 330 $JK^{-1}kg^{-1}$ can be taken as the heat capacity value of PBZ thin film. The theoretical density ρ of PBZ thin film with the pseudocubic structure can be determined to be 7.7 gcm^{-3} by using the software JADE. Using Eq. (1) and Eq. (2), ΔT and ΔS at selected electric fields are presented in **Fig. 3(a)** and (b) and in the insets of Fig. 3(a) and (b), respectively. Peak ΔT = 45.3 °C at 598 $kVcm^{-1}$ was obtained at 290 K (see Fig. 3(a)), as well as peak ΔS = 46.9 $JK^{-1}kg^{-1}$ (see inset of Fig.3(a)).

For comparison, **Table 1** lists the ECE characteristics of PBZ, $PbZr_{0.95}Ti_{0.05}O_3$,[1] P(VDF-TrFE)55/45,[2,3] $PbSc_{0.5}Ta_{0.5}O_3$,[24] PMN-PT90/10,[23] and $Pb(Mg_{1/3}Nb_{2/3})_{0.65}Ti_{0.35}O_3$ thin films.[6] Obviously, the ΔT, $\Delta T/\Delta E$ and $\Delta T \cdot \Delta S$ of PBZ thin film are the biggest among all of them, except the ΔS (60 $JK^{-1}kg^{-1}$ for P(VDF-TrFE)55/45). The large $\Delta T \cdot \Delta S$ value (2125 Jkg^{-1}) of PBZ thin film at room temperature means large refrigerant capacity (RC), which is particularly required in cooling systems. Moreover, peak ΔT = 45.3 K at 598 $kVcm^{-1}$, represents a peak energy change $C \cdot \Delta T$ = 14.95 $kJkg^{-1}$, and the corresponding hysteresis loss taken near the peak (T_{ECE} = 293 K) was about 5.5% of the energy change. Hysteresis losses have the potential to reduce the peak ECE temperature change by only 2.5 K. Hysteresis

losses may be reduced[25] by (i) reducing the measurement frequency, (ii) introducing chemical substituents, and (iii) modifying microstructures.

Twin-peak ECE with maximum ΔT < 5 °C (Fig. 3(b)) and ΔS < 4.5 $JK^{-1}kg^{-1}$ (inset of Fig. 3(b)) were observed. Such twin-peak ECE also have been reported in several perovskite relaxors.[26-29] The appearance of the twin peak can be explained with the field-induced polar nanodomain formation and alignment of these polar species.[30] The low-temperature peak and the high-temperature peak of the twin peaks correspond to the depolarization temperature (T_{dp}) and the Curie temperature,[31,32] respectively.

In order to elucidate the giant ECE in PBZ thin film, the pyroelectric coefficients $(\partial P/\partial T)_E$ at selected electric fields are plotted in Fig. 3(c) and (d). It is clear from Fig. 3(c) that with the increase of the electric field, the $(\partial P/\partial T)_E$ around the temperature of the peak first increases and reaches a maximum at 210 $kVcm^{-1}$, and then decreases. Likewise, in Fig. 3(d), the $(\partial P/\partial T)_E$ near and between the temperature of the twin-peak first increases and reaches a maximum at 100 $kVcm^{-1}$, and then decreases.

To get an insight into this phenomenon, *P-E* loops under different electric fields and the dc electric field dependence of the permittivity ($\varepsilon(E)$) were investigated at 293 K and 403 K. Double *P-E* loops were visible at 293 K when the electric field is lower than 210 $kVcm^{-1}$, as shown in the inset of Fig. 3(c), indicating that an electric field induced AFE-FE phase transition takes place.[33,34] Typical ferroelectric *P-E* loops were obtained when the electric field is higher than 210 $kVcm^{-1}$, as shown in Fig. 2(b). In contrast, only ferroelectric *P-E* loops can be obtained at 403 K under all electric fields, as shown in the inset of Fig. 3(d). A peak in the curve of $\varepsilon(E)$ (inset of Fig. 3(c)) was observed at 293 K, which further revealed the existence of the electric field induced AFE-FE phase transition.[33,34] No peak can be detected in the curve of $\varepsilon(E)$ (inset of Fig. 3(d)) at 403 K. From the above analysis, it can be inferred that the giant EC at room temperature for PBZ thin film may be caused by the electric

field-induced AFE-FE phase transition, which could induce new ways to enhance the electrocaloric efficiency by virtue of the noncollinearity between the electric field and the polarization.[7] It is well known that for second order phase transition or higher order phase transition, the entropy change ΔS is normally smaller than first order phase transition. Bhadra et al.[8] carried out a high temperature X-ray study of structure phase transitions in $Pb_{1-x}Ba_xZrO_3$ powders and confirmed the first order nature of the A_O to F_R transition. The A_O to F_R transition is similar to the austensite (A) to martensite (M) transition[8] in some alloys, and large ΔS can be caused during the transition. Previous work[31,32] pointed out that latent heat (or ΔS) from the field-induced phase transition can significantly contribute to the ECE below the depolarization temperature T_{dp}. Therefore, the giant ECE at room temperature for PBZ thin film can be attributed to the contribution of the electric field induced A_O to F_R transition. However, the transition of AFE to FE phases may not be the only reason responsible for the large ECE in PBZ system. Orientation of nanoregions existed in the thin film under electric field may also contribute to this giant ECE because a large entropy change from totally random nanoregions to ordered nanoregions occurs. The effect of orientation of nanoregions induced by electric field on ECE is under investigation.

Moreover, the latest work of Zhang. et al.[35] showed that large ECE can be obtained in materials with an invariant critical point (ICP), where multiphase coexistance and large entropy change ΔS can be obtained during the phase transition. As a relaxor with the structure of nano-scaled O_{AF} phase and R_F phase coexisted, the PBZ thin film with giant ECE at room temperature can be assumed as a material with a ICP. For this, further theoretical research is needed to be done.

Figure 3. (a) and (b) ΔT of PBZ film at selected electric fields, the inset is ΔS ; (c) and (d) $(\partial P/\partial T)_E$ of PBZ film at selected electric fields, the inset is *P*-*E* loop and $\varepsilon(E)$ measured at 293 K and 403 K.

Table 1. Electrocaloric characteristics of thin films.

3. Conclusions

Giant ECE (ΔT = 45.3 K and ΔS = 46.9 $JK^{-1}kg^{-1}$ at 598 $kVcm^{-1}$) at room temperature (290 K) rather than at the Curie temperature (408 K) was obtained in the antiferroelectric and ferroelectric phases coexisted relaxor $Pb_{0.8}Ba_{0.2}ZrO_3$ thin film fabricated on $Pt(111)/TiO_x/SiO_2/Si$ substrate by sol-gel method. Field-induced nano-scaled antiferroelectric to ferroelectric phase transition played a key role in the dramatic EC effect. The PBZ thin film can be used as a promising material for applications in cooling systems near room temperature.

4. Experimental procedure

Fabrication: $Pb_{80}Ba_{20}ZrO_3$ (PBZ) thin film was fabricated by a sol-gel method. $Pb(OAc)_2 \cdot 3H_2O$ and $Ba(OAc)_2$ were dissolved in glacial acetic and deionized water. In order to compensate the Pb loss during sintering, 20% excess Pb was added. Separately, acetylacetone was added to a mixture of $Zr(O^nPr)_4$ and 2-methoxyethanol and the resulting solution was stirred at room temperature for 30 min. The Pb/Ba and Zr solutions were mixed and stirred at room temperature for 2 h. The final concentration of the synthesized PBZ sol was 0.3M. After aging the sol for 24 h. PBZ sols were passed through a 0.2 μm filter for spin coating at 4000 rpm for 30 s onto $Pt(111)/TiO_x/SiO_2/Si(100)$ substrates that were rinsed with acetone and 1-propanol. Each layer was pyrolized at 350 °C for 3 min and then heated at 550 °C for 5 min on hotplates. After the deposition of 8 layers, the film was annealed in a tube furnace at 750 °C for 30 min in air. The final thickness of the film was about 320 nm. 150×150 μm^2 top electrodes of Cr/Au were deposited by thermal evaporation.

Characterization: The PBZ film structure was monitored by X-ray diffraction (XRD; Bruker-AXS D5005, Siemens, Munich, Germany) on a diffractometer, using Cu Kα radiation (λ=1.5406Å). The surface morphology of the film was examined by scanning electron

microscope (SEM; FEI XL30 SFEG, Philips, Edihoven, The Netherlands). The microstructure of the film was studied by transmission electron microscopy (TEM; CM20, Philips, Edihoven, The Netherlands). Dielectric permittivity measurements were carried out using an impedance analyzer (Wayne-Kerr Electronics, UK) at V = 100 mV. Electric dependences of polarization hysteresis (*P-E*) loop and leakage current (*I-E*) were obtained by means of a ferroelectric tester (RT66A, Radiant Technologies Inc., Albuquerque, NM, USA). Temperature was controlled with the aid of a Peltier element.

Acknowledgements

Peng would like to thank National Natural Science Foundation (51172187), the SPDRF (20116102130002) and 111 Program (B08040) of MOE, the Xi'an Science and Technology Foundation (CX1261-2, CX1261-3) of China, and China Scholarship Council for personel financial support for working in Cranfield.

Received: ((will be filled in by the editorial staff))
Revised: ((will be filled in by the editorial staff))
Published online: ((will be filled in by the editorial staff))

[1] A. S. Mischenko, Q. Zhang, J. F. Scott, R. W. Whatmore, N. D. Mathur, *Science* **2006**, *311*, 1270.

[2] Sheng-Guo Lu, Qiming Zhang, *Adv. Mater.* **2009**, *21*, 1983.

[3] Bret Neese, Baojin Chu, Sheng-Guo Lu, Yong Wang, E. Furman, Q. M. Zhang, *Science* **2008**, *321*, 821.

[4] O. V. Pakhomov, S. F. Karamenko, A. A. Semenov, A. S. Starkov, A. V. Es'kov, *Tech. Phys.* **2010**, *55*, 1155.

[5] B. A. Tuttle, D. A. Payne, *Ferroelectrics* **1981**, *37*, 603.

[6] D. Saranya, A.R. Chaudhuri, J. Parui, S.B. Krupanidhi, *Bull. Mater. Sci.* **2009**, *32*, 259.

[7] I. Ponomareva, S. Lisenkov, *Phys. Rev. Lett.* **2012**, *108*, 167604.

[8] Bhadra P. Pokharel, Dhananjai Pandey, *J. Appl. Phys.* **2001**, *90*, 2985.

[9] L. Pintilie, I. Boerasu, M.J.M. Gomes, M. Pereira, *Thin Solid Films* **2004**, *458*, 114.

[10] Xihong Hao, Jiwei Zhai, Xiujian Chou, Xi Yao, *Solid State Commun.* **2007**, *142*, 498.

[11] Ebru Mensur Alkoy, Sedat Alkoy, Tadashi Shiosaki, *Japan J. Appl. Phys.* **2005**, *44*, 6654.

[12] Dwight Viehland, *Phys. Rev. B* **1995**, *52*, 778.

[13] Satyendra Singh, S. B. Krupanidhi, *J. Appl. Phys.* **2012**, *111*, 024314.

[14] J. Ricote, R. W. Whatmore, D. J. Barber, *J. Phys.: Condens. Matter* **2000**, *12*, 323.

[15] Bhadra P. Pokharel, Dhananjai Pandey, *J. Appl. Phys.* **2000**, *88*, 5364.

[16] Bhadra P. Pokharel, Dhananjai Pandey, V. Siruguri, S. K. Paranjpe, *Appl. Phys. Lett.* **1999**, *74*, 756.

[17] N. A. Pertsev, A. G. Zembilgotov, A. K. Tagantsev，*Phys. Rev. Lett.* **1998**, *80*, 1988.

[18] S. P. Alpay, I. B. Misirlioglu, A. Sharma, Z.-G. Ban，*J. Appl. Phys.* **2004**, *95*, 8118.

[19] G. Akcay, S. P. Alpay, J. V. Mantese, G. A. Rossetti，*Appl. Phys. Lett.* **2007**, *90*, 252909.

[20] J. Zhang, S. P. Alpay, G. A. Rossetti，*Appl. Phys. Lett.* **2011**, *98*, 132907.

[21] G. Akcay, S. P. Alpay, G. A. Rossetti, J. F. Scott，*J. Appl. Phys.* **2008**, *103*, 024104.

[22] T. M. Correia, J. S. Young, R. W. Whatmore, J. F. Scott, N. D. Mathur, Q. Zhang, *Appl. Phys. Lett.* **2009**, *95*, 182904.

[23] A. S. Mischenko, Q. Zhang, R. W. Whatmore, J. F. Scott, N. D. Mathur, *Appl. Phys. Lett.* **2006**, *89*, 242912.

[24] T. M. Correia, S. Kar-Narayan, J. S. Young, J. F. Scott, N. D. Mathur, R. W. Whatmore, Q. Zhang, *J. Phys. D: Appl. Phys.* **2011**, *44*, 165407.

[25] D. Viehland, J. F. Li, *J. Appl. Phys.* **2011**, *89*, 1826.

[26] Juha Hagberg, Antti Uusimäki, Heli Jantunen, *Appl. Phys. Lett.* **2008**, *92*, 132909.

[27] J. Peräntie, J. Hagberg, A. Uusimäki, H. Jantunen, *Phys. Rev. B* **2010**, *82*, 134119.

[28] Matjaz Valant, Lawrence J. Dunne, Anna-Karin Axelsson, Neil McN. Alford, George Manos, Jani Peräntie, Juha Hagberg, Heli Jantunen, Antoni Dabkowski, *Phys. Rev. B* **2010**, *81*, 214110.

[29] L. Shebanovs, K. Borman, W. N. Lawless, A. Kalvane, *Ferroelectrics* **2002**, *273*, 137.

[30] L. J. Dunne, M. Valant, A. K. Axelsson, G. Manos, N. M. Alford, *J Phys D: Appl. Phys.* **2011**, *44*, 375404.

[31] G. C. Lin, X. M. Xiong, J. X. Zhang, Q. Wei, *J. Therm. Anal. Calorim.* **2005**, *81*, 41.

[32] G. Sebald, S. Pruvost, L. Seveyrat, L. Lebrun, D. Guyomar, B. Guiffard, *J. Eur. Ceram. Soc.* **2007**, *27*, 4021.

[33] Yaoyang Liu, Xiaomei Lu, Yaming Jin, Song Peng, Fengzhen Huang, Yi Kan, Tingting Xu, Kangli Min, Jinsong Zhu, *Appl. Phys. Lett.* **2012**, *100*, 212902.

[34] T. M. Correia, Q. Zhang, *J. Appl. Phys.* **2010**, *108*, 044107.

[35] Z. K. Liu, Xinyu Li, Q. M. Zhang, *Appl. Phys. Lett.* **2012**, *101*, 082904.

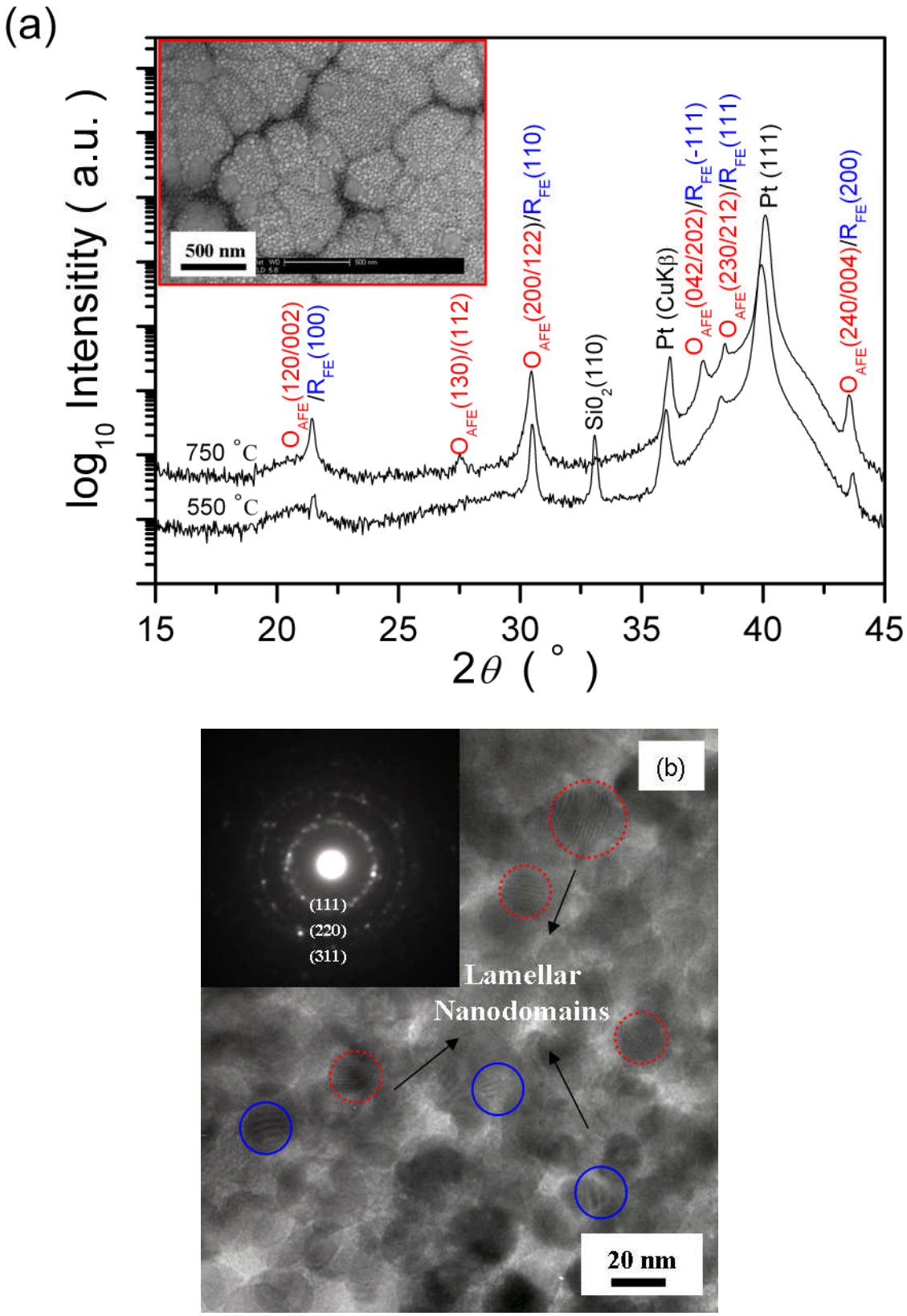

Figure 1. (a) XRD patterns and SEM surface image (inset) of the PBZ thin film; (b) TEM image and SAED pattern (inset).

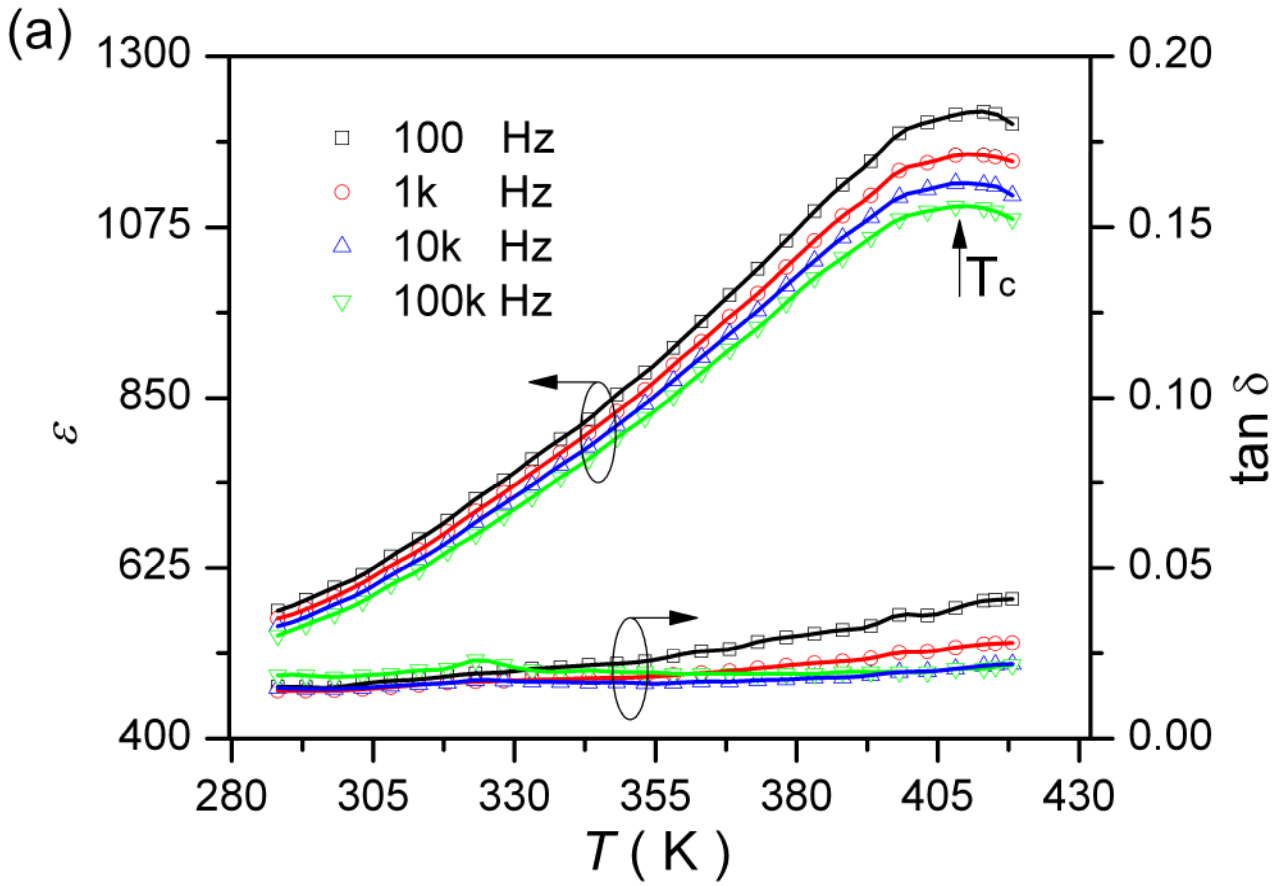
(a)
100 Hz
1k Hz
10k Hz
100k Hz
Tc
ε
tan δ
T (K)

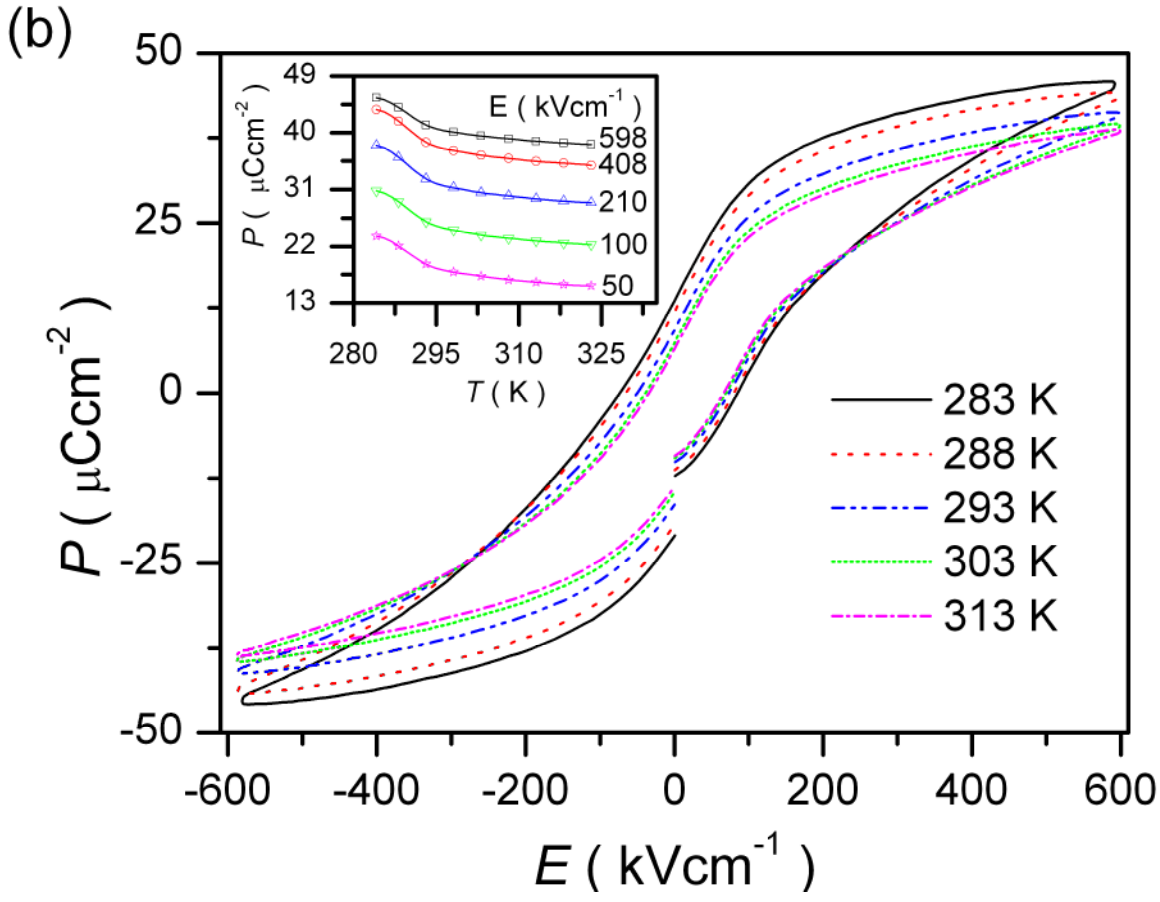
(b)
P (μCcm-2)
E (kVcm-1)
283 K
288 K
293 K
303 K
313 K
E (kVcm-1)
598
408
210
100
50
T (K)

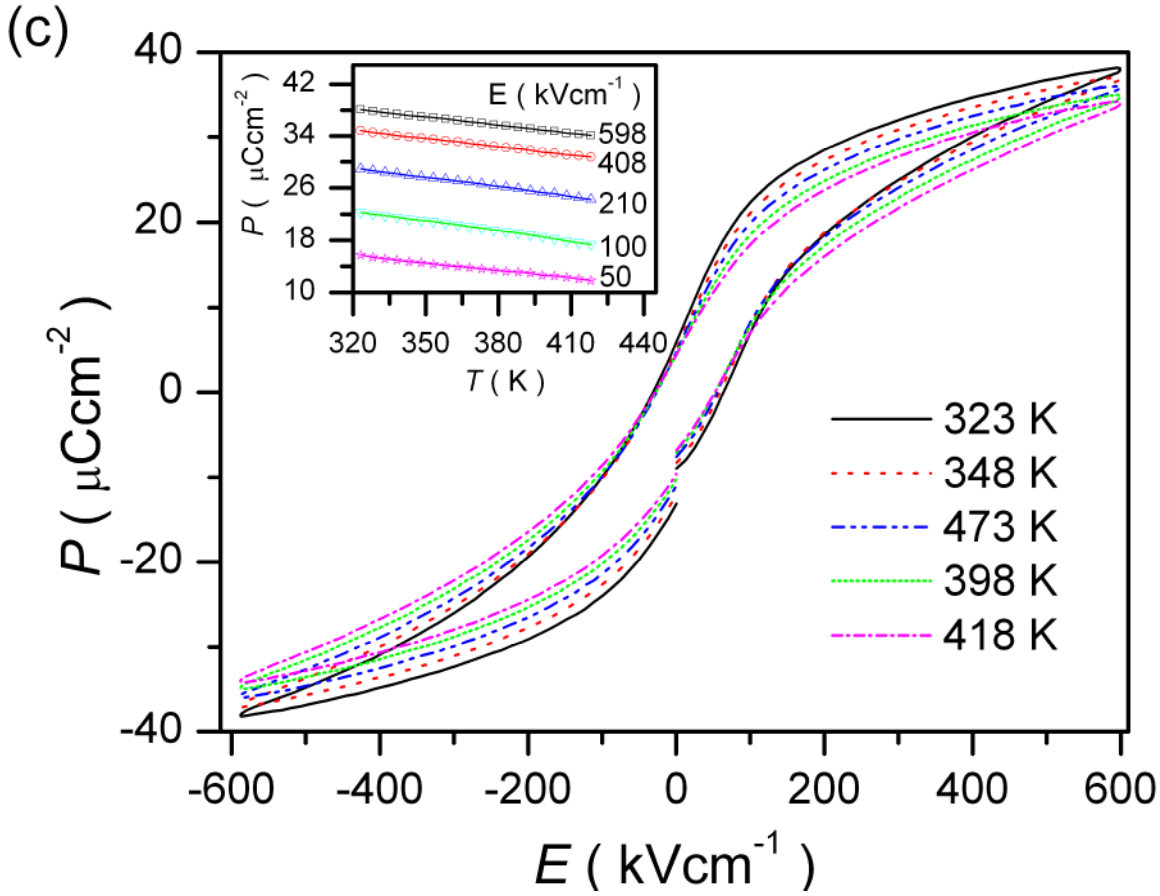
(c)
P (μCcm-2)
E (kVcm-1)
323 K
348 K
473 K
398 K
418 K
P (μCcm-2)
T (K)
E (kVcm-1)
598
408
210
100
50

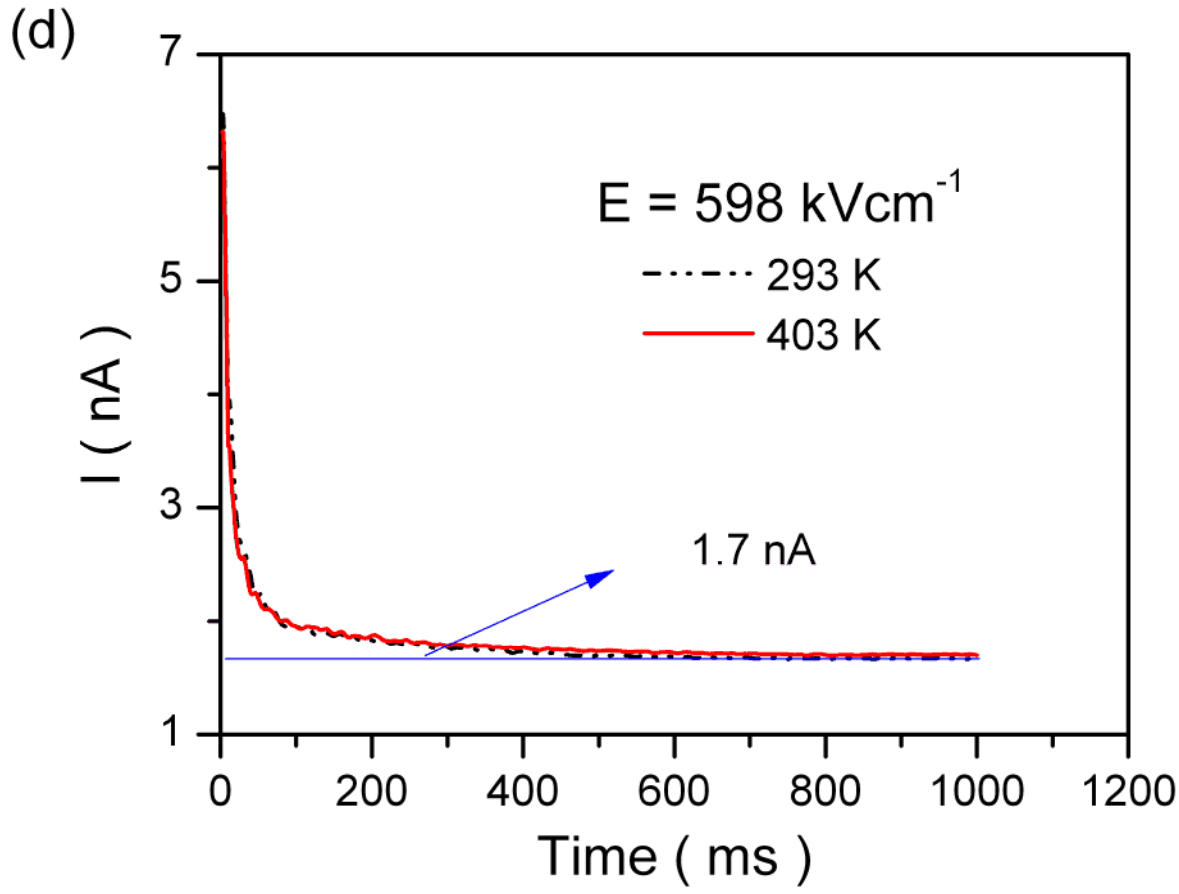
(d)
I (nA)
Time (ms)
E = 598 kVcm-1
293 K
403 K
1.7 nA

Figure 2. (a) $\varepsilon(T)$ and tan $\delta(T)$ of PBZ thin film; (b) and (c) *P-E* loops at selected temperatures, the inset is $P(T)$ at selected electric field values ; (d) leakage current $I(t)$.

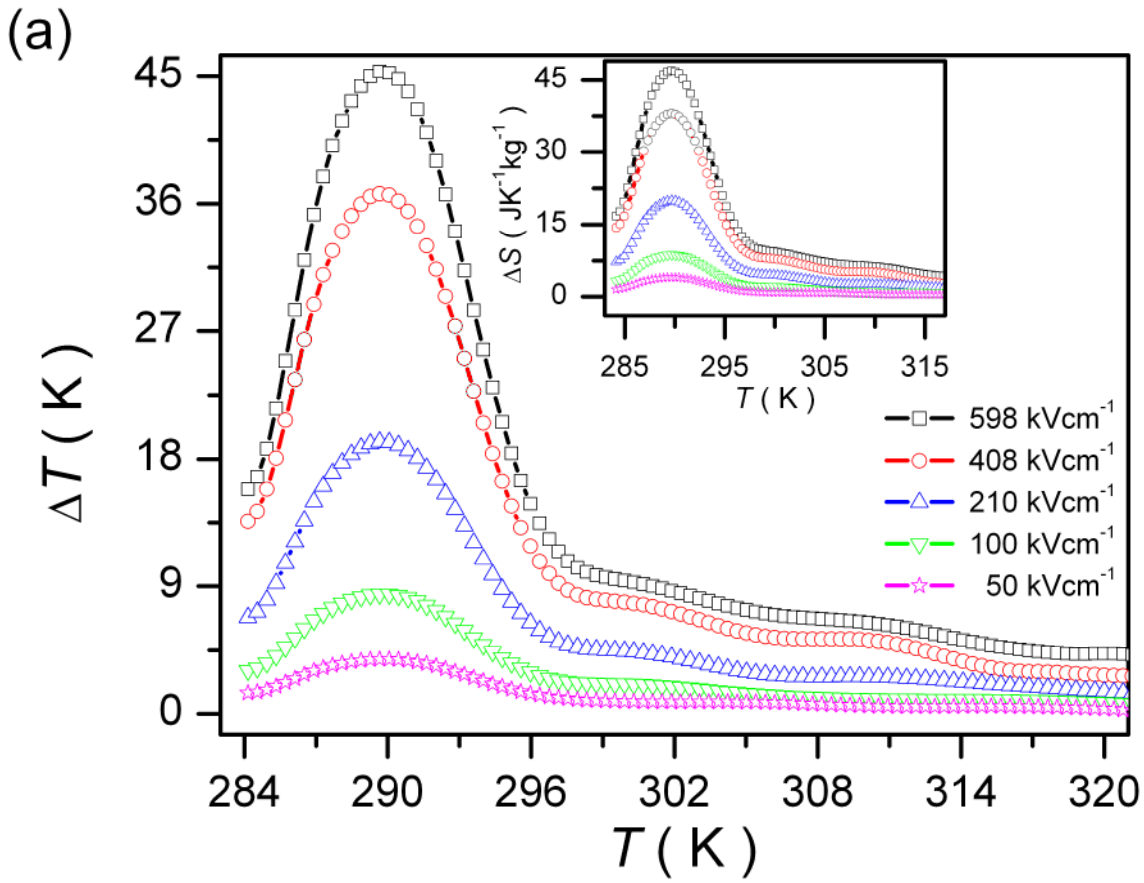

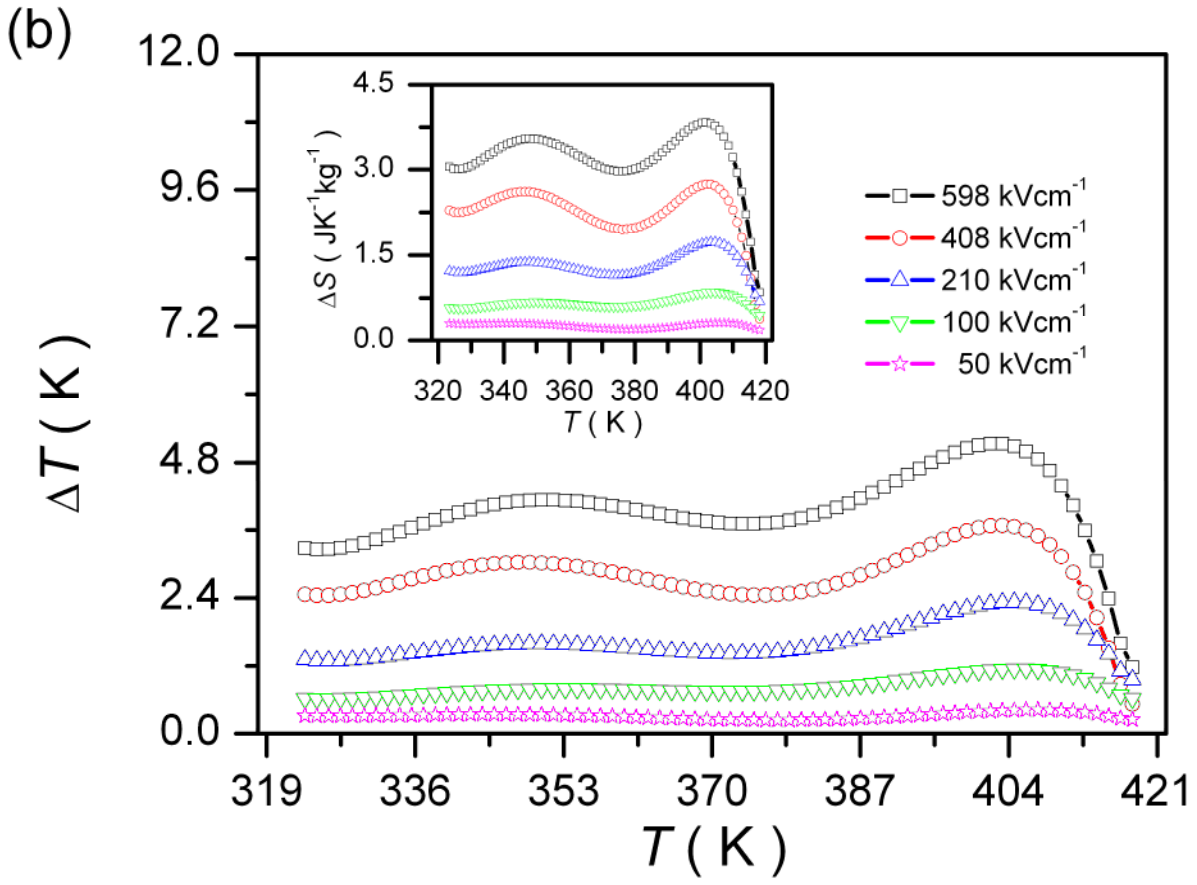
(b)
ΔT (K)
T (K)
ΔS (JK-1kg-1)
598 kVcm-1
408 kVcm-1
210 kVcm-1
100 kVcm-1
50 kVcm-1

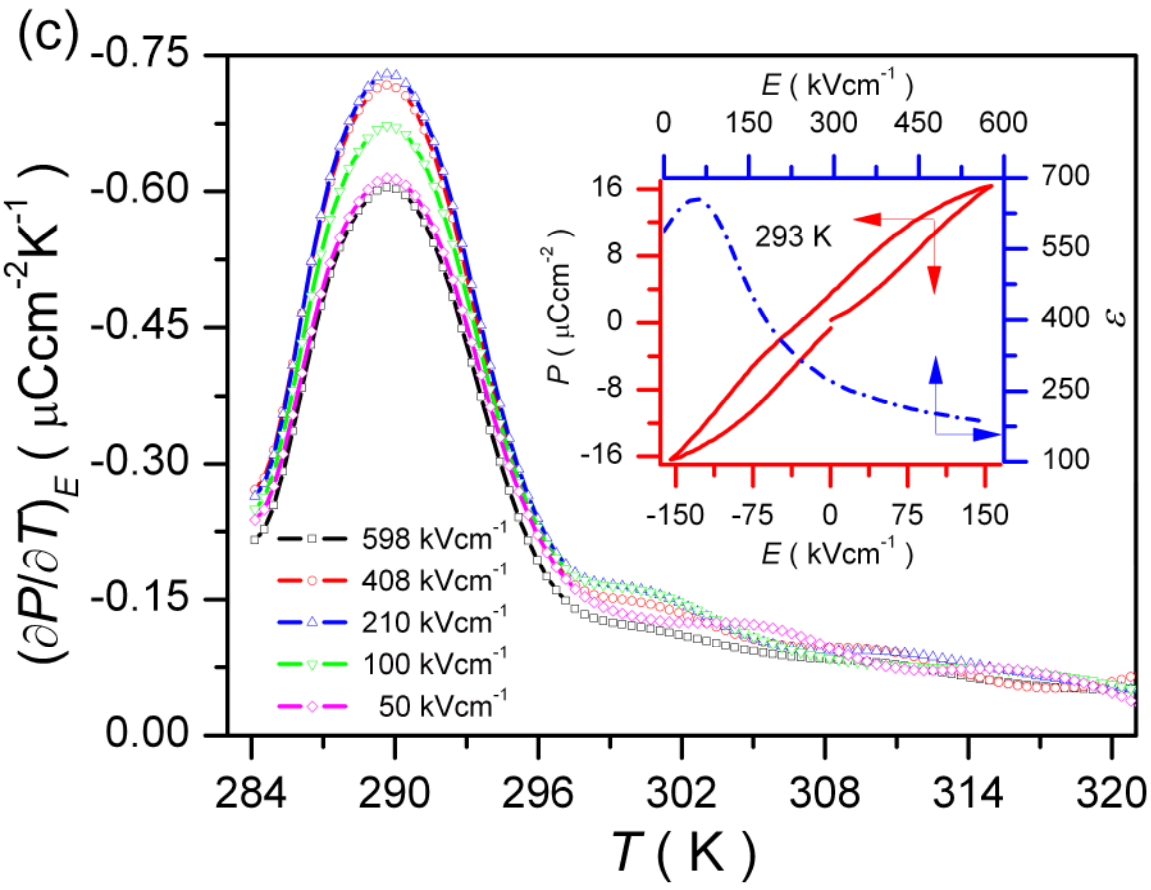
(c)
(∂P/∂T)E (μCcm-2K-1)
T (K)
598 kVcm-1
408 kVcm-1
210 kVcm-1
100 kVcm-1
50 kVcm-1
E (kVcm-1)
P (μCcm-2)
293 K
ε

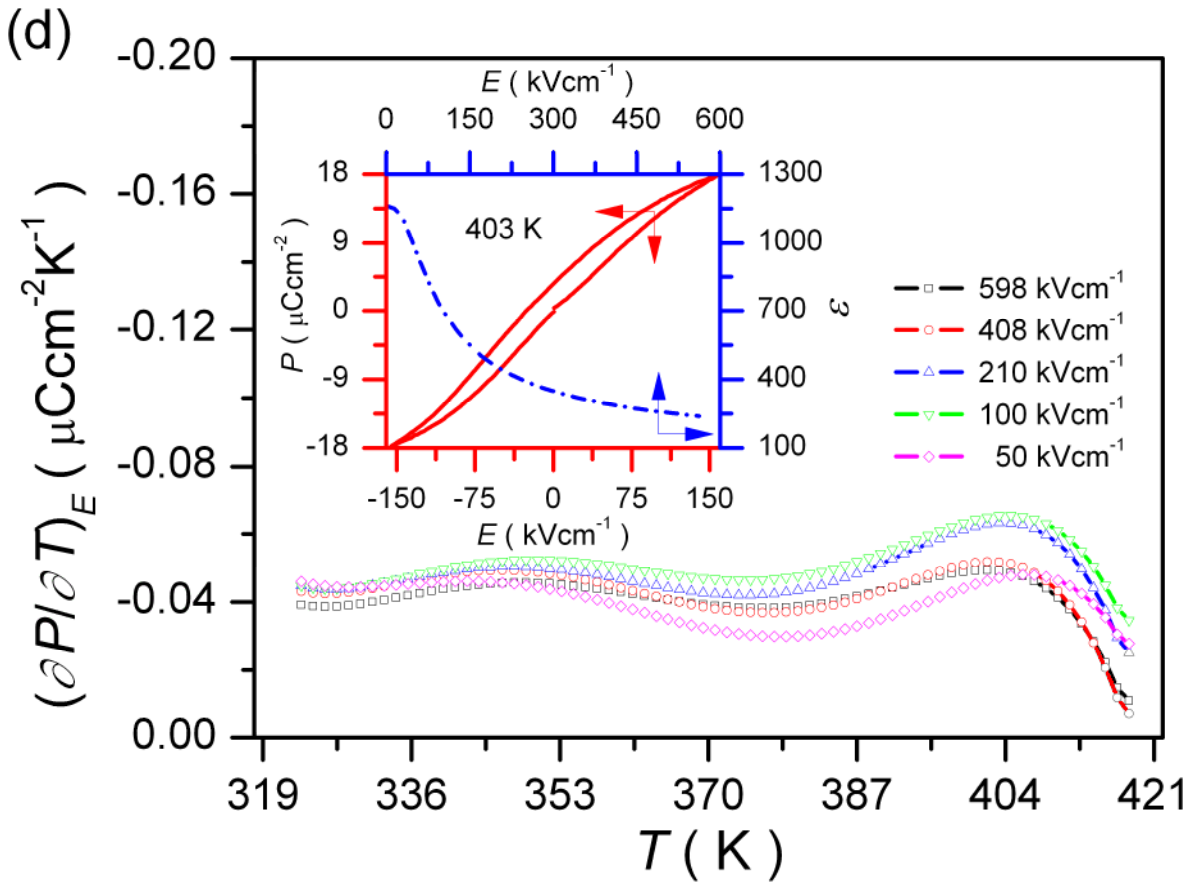

Figure 3. (a) and (b) ΔT of PBZ film at selected electric fields, the inset is ΔS ; (c) and (d) $(\partial P/\partial T)_E$ of PBZ film at selected electric fields, the inset is *P*-*E* loop and $\varepsilon(E)$ measured at 293 K and 403 K.

Table 1. Electrocaloric characteristics of thin films.

Material	T (°C)	ΔT (°C)	ΔE (kVcm^{-1})	$\Delta T/\Delta E$ (K cmkV^{-1})	ΔS (JK^{-1}kg^{-1})	$\Delta T \cdot \Delta S$ (Jkg^{-1})
$Pb_{80}Ba_{20}ZrO_3$	17	45.3	598	0.076	46.9	2125
$PbZr_{0.95}Ti_{0.05}O_3$[1]	222	12	776	0.015	8	96
P(VDF-TrFE)55/45[2,3]	80	12.6	2090	0.006	60	756
$PbSc_{0.5}Ta_{0.5}O_3$[20]	68	6.2	774	0.008	6.3	39
PMN-PT90/10[19]	75	5	895	0.006	5.6	28
$(Pb_{0.88}La_{0.08})(Zr_{0.65}Ti_{0.35})O_3$[7]*	45	40	1250	0.032	41.5	1660
$Pb(Mg_{1/3}Nb_{2/3})_{0.65}Ti_{0.35}O_3$[6]	140	31	747	0.041	32	992

* Direct temperature reading.

Giant ECE (ΔT = 45.3 K and ΔS = 46.9 $JK^{-1}kg^{-1}$ at 598 $kVcm^{-1}$) at room temperature (290 K) rather than at the Curie temperature (408 K) can be obtained in the antiferroelectric and ferroelectric phases coexisted relaxor $Pb_{0.8}Ba_{0.2}ZrO_3$ thin film, which makes PBZ a promising material for applications in cooling systems near room temperature.

Keyword: $Pb_{0.8}Ba_{0.2}ZrO_3$ thin film; relaxor; field-induced; electrocaloric effect

By *Biaolin Peng*, *Huiqing Fan** and *Qi Zhang**

Giant electrocaloric effect in nano-scaled antiferroelectric and ferroelectric phases coexisted relaxor $Pb_{0.8}Ba_{0.2}ZrO_3$ thin film at room temperature

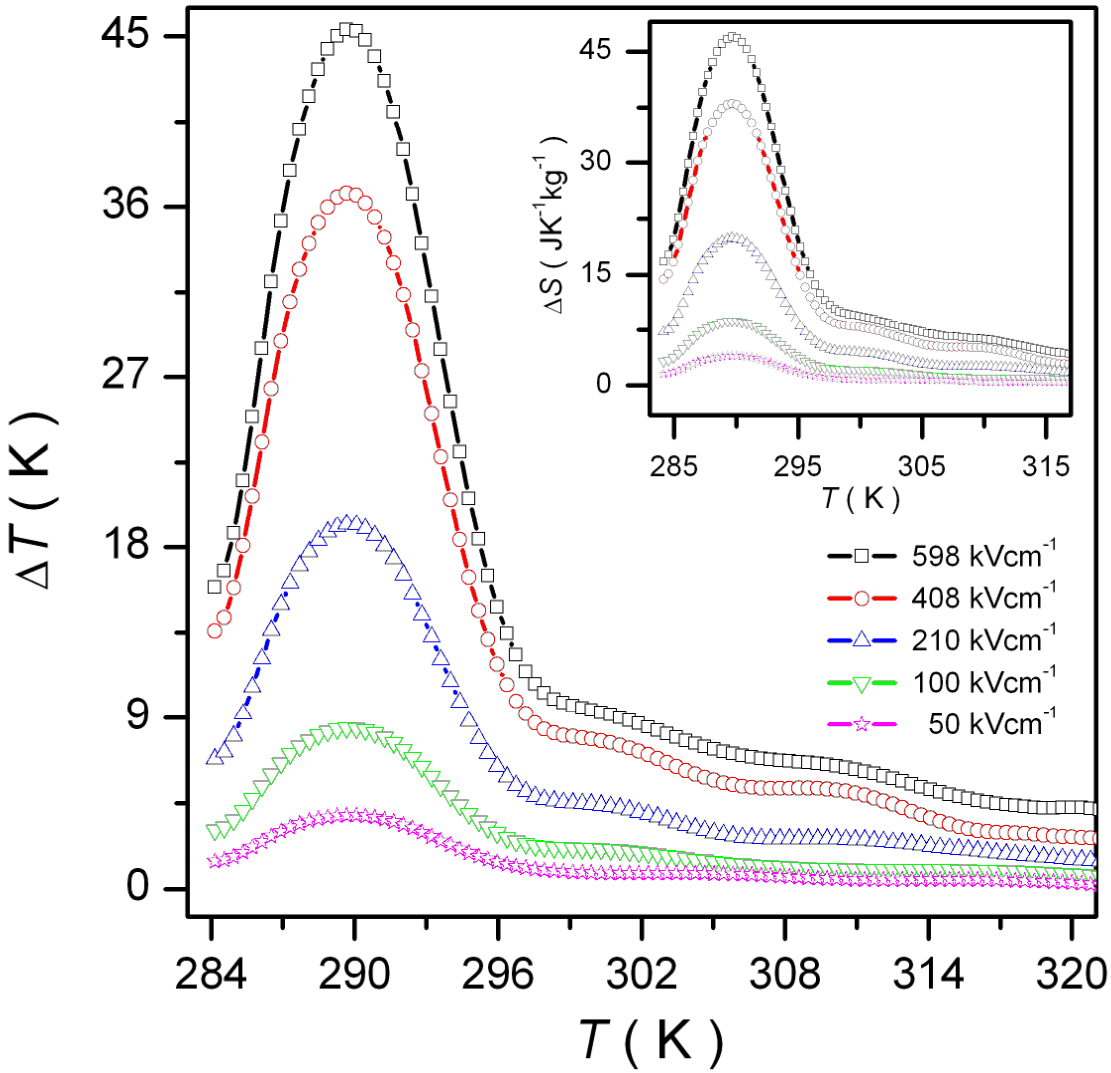

A giant electrocaloric effect in nanoscale antiferroelectric and ferroelectric phases coexisting in a relaxor Pb0.8Ba0.2ZrO3 thin film at room temperature

Peng, Biaolin

2013-06-20T00:00:00Z

The definitive version is available at www3.interscience.wiley.com

Biaolin Peng, Huiqing Fan, Qi Zhang, A giant electrocaloric effect in nanoscale antiferroelectric and ferroelectric phases coexisting in a relaxor Pb0.8Ba0.2ZrO3 thin film at room temperature, Advanced Functional Materials, Volume 23, Issue 23, 20 June 2013, Pages 2987–2992.

http://dx.doi.org/10.1002/adfm.201202525